Position estimation delays in signal injection-based sensorless PMSM drives

F. Cupertino, A. Guagnano, A. Altomare
DEE
Politecnico di Bari
Bari, Italy

G. Pellegrino
DENERG
Politecnico di Torino
Torino, Italy

Abstract: **The causes of position estimation delays and their effects on the sensorless control of permanent magnet synchronous motor drives are investigated. The position of a permanent magnet synchronous machine is estimated via the injection of high frequency voltage signals. The delays under investigation are due to the digital implementation of the control algorithm and to the digital filters adopted for decoupling the inspection signals from the fundamental components of the stator current measures. If not correctly modeled and compensated, such delays can reduce the performance of the control scheme. Experimental results are provided, proving the accuracy of the modeling approach and the effectiveness of the related compensation strategy.**

***Index Terms*—Sensorless control, Permanent magnet machines, Motor drives, Motion control, Position control, Digital filters, Phase-locked loops, State observers.**

I. Introduction

The rotor position information is necessary for vector control of AC machines, for coordinate transformations to and from the synchronous reference frame and the feedback signal of closed loop position and speed control. In many industrial applications, the position sensor may be the cause of several disadvantages in terms of cost, reliability of the drive system, need for maintenance and noise interference.

For all those reasons, there has been much research on sensorless techniques, that can estimate the rotor position from the measure of electrical quantities only and do not require any position sensor on the machine shaft.

To overcome the limitations of model-based observers at zero and very low speed and their sensitivity to motor parameters variations [1], the methods that utilize the magnetic saliency of the motor have been intensively studied over the last two decades [2]. Although techniques that do not require low pass filtering of the motor currents have been proposed [3], the simplest approaches to position sensorless control at low speed are still based on the injection of a sinusoidal, high frequency voltage signal, either rotating in the stationary reference frame [4], or pulsating along the direct axis of the observed synchronous reference frame [5]. Other methods inject current signals instead of voltages, but still cannot avoid the need for filtering the inspection signals [6]. Advantages and disadvantages of rotating and pulsating voltage injection techniques have been thoroughly discussed [7-8], and both the techniques are widely adopted, in practice.

In this paper the effect of all delays related to the digital implementation of a position estimation algorithm are investigated, with reference to two control schemes, one having rotating voltage signal injection and the other one with pulsating voltage injection. The actuation delay and the phase delays due to filtering of the inspection currents have negative effects over the accuracy of the position estimation, as expected. Such effects are modeled and quantified, and finally compensated. The results of the study can be extended to the schemes based on pulsating signals injection, either voltage-based or current-based.

A description of the position observer and the proposed compensation scheme are reported in section II for the rotating injection case and in section III for the pulsating injection case, respectively. Experimental results are reported at section IV, referring to a test permanent magnet synchronous motor (PMSM), for servo application.

II. Rotating Voltage Carrier

A voltage vector, rotating with pulsation ω_{inj}, is added to the voltage reference signals given by the current regulators [4]. The injected voltage expression, in the stationary α-β reference frame, is the one in (1):

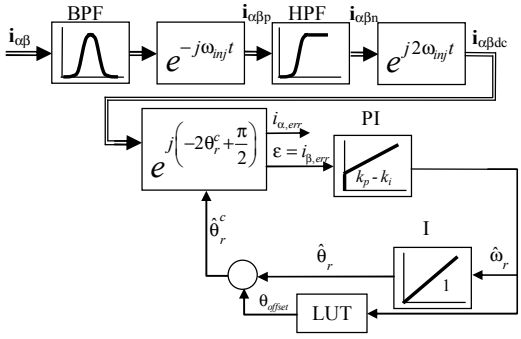

Fig. 1- Tracking observer used with rotating voltage injection scheme, and feed-forward compensation of all delays via a look-up table.

$$\bar{u}_{\alpha\beta,inj} = U_{inj} \cdot e^{j\omega_{inj}t} = U_{inj}\cos(\omega_{inj}t) + jU_{inj}\sin(\omega_{inj}t) \quad (1)$$

The high frequency stator currents, given in (2) in complex form, can be calculated assuming that the voltage drop across the motor resistance is negligible and reminding that the electro-motive force due to PM magnet flux linkage has no component in the high frequency motor model:

$$\bar{\imath}_{\alpha\beta,inj} = {i_{inj}}^{p} \cdot e^{j\left(\omega_{inj}t-\frac{\pi}{2}\right)} - {i_{inj}}^{n} \cdot e^{-j\left(\omega_{inj}t-2\theta_r-\frac{\pi}{2}\right)} = {\bar{\imath}_{inj}}^{p} + {\bar{\imath}_{inj}}^{n} \quad (2)$$

Position information, carried by the negative sequence current component, can be extracted using the tracking observer shown in figure 1. The band-pass filter (BPF) isolates the current components at injection frequency while the high-pass filter (HPF) removes the positive sequence current component in (2). The so isolated negative sequence component is manipulated by coordinates transformation to calculate the error signal (3):

$$\varepsilon = \mathcal{I}m\{\bar{\imath}_{\alpha\beta\_err}\} = {i_{inj}}^{n} sin(2\theta_r - 2\hat{\theta}_r) \cong {i_{inj}}^{n}(2\theta_r - 2\hat{\theta}_r) \quad (3)$$

that is the input of the position tracking loop. The pulsation of the negative sequence component in (2) is equal to ω_{inj}-$2\omega_r$ depends on motor speed. The phase contribution of both BP- and HP-filter stages at such pulsation is generally different from zero and introduces an estimation error. Moreover, the delays due to the inverter and to the digital implementation of the control scheme have to be taken into account. Last, the phase of the motor impedance at the injection frequency could be different from being exactly π/2, due to core and PM loss. This implies that the actual error signal is a function of the filters response and the other additional delays:

$$\varepsilon = {i_{inj}}^{n}{M_{BPF}}^{n}{M_{HPF}}^{n} sin\left(2(\theta_r - \hat{\theta}_r) + {f_{BPF}}^{n} + {f_{HPF}}^{n} + \theta_{dgt}\right) \quad (4)$$

where

- ${M_{BPF}}^{n}$ and ${f_{BPF}}^{n}$ are the amplitude and phase of the BPF at $\omega_{inj} - 2\omega_r$;
- ${M_{HPF}}^{n}$ and ${f_{HPF}}^{n}$ are the amplitude and phase of the HPF at $2\omega_{inj} - 2\omega_r$;
- θ_{dgt} is the phase delay due to the inverter and to the digital implementation of the control scheme.

It has to be remarked that the all the phase contributions are applied to a negative sequence component, then phase lags are added and, vice versa, phase leads are subtracted in (4). The estimation error can be compensated by adding a position offset at the estimated motor position:

$$\theta_{offset} = -\frac{{f_{BPF}}^{n} + {f_{HPF}}^{n} + \theta_{dgt}}{2} \quad (5)$$

This position offset varies with the motor speed and can be stored in a look-up table (LUT), as shown in figure 1.

III. Pulsating Voltage Carrier

When pulsating voltage injection is adopted, a sinusoidal voltage $u_{d,inj}=U_{inj}\ sin(\omega_{inj}t)$ is added to the *d*-axis reference voltage, that is at the output of the *d*-current regulator. As reported in figure 2, the high frequency currents components are extracted from measured currents by means of a BPF, then they are rotated towards the estimated rotor reference frame, where the product of real and imaginary current components is calculated and finally low-pass filtered. In the ideal case of no delay introduced by the BPF, the output of the LPF is proportional to the sine of the position estimation error:

$$LPF\{\varepsilon\} = -2{i_{inj}}^{2} sin(2\theta_{err}) \cong -4{i_{inj}}^{2}\theta_{err} \quad (6)$$

where i_{inj} is the amplitude of the high frequency current and θ_{err} is the position estimation error. If the BPF amplitude and phase error is considered, equation (6) becomes:

$$\begin{aligned} LPF\{\varepsilon\} = -{i_{inj}}^{2}\big[&(L_s/\Delta L_s){M_{BPF}}^{p}{M_{BPF}}^{n} sin({f_{BPF}}^{p} + {f_{BPF}}^{n} - \pi) \\ &+ 2{M_{BPF}}^{p}{M_{BPF}}^{n} sin(2\theta_{err} + {f_{BPF}}^{p} + {f_{BPF}}^{n}) \\ &+ (\Delta L_s/L_s){M_{BPF}}^{p}{M_{BPF}}^{n} sin(4\theta_{err} + {f_{BPF}}^{p} + {f_{BPF}}^{n} + \pi)\big] \end{aligned} \quad (7)$$

$LPF\{\varepsilon\}$ given in (7) is not an adequate error signal since it is not zero when the position estimation error is zero. To overcome this problem a compensated $\hat{\theta}_r^c$ rotor position is introduced, adding to the estimated position $\hat{\theta}_r$ an offset position θ_{offset}. In the compensated reference frame the $LPF\{\varepsilon\}$ becomes

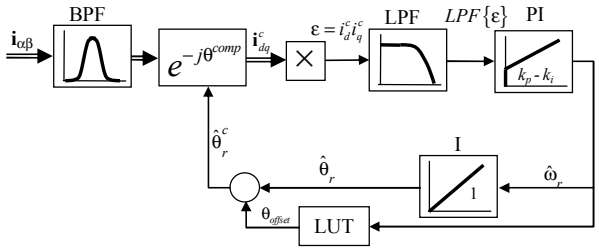

Fig. 2- Tracking observer used with pulsating voltage injection scheme and feed-forward compensation of the BPF delays via a look-up table.

$$
\begin{aligned}
&LPF(\varepsilon) \\
&= -{i_{inj}}^2\big[(L_s/\Delta L_s){M_{BPF}}^p{M_{BPF}}^n sin\big({f_{BPF}}^p \\
&\qquad + {f_{BPF}}^n - \pi - 2\theta_{offset}\big) \\
&\quad + 2{M_{BPF}}^p{M_{BPF}}^n sin\big(2\theta_{err} + {f_{BPF}}^p \\
&\qquad + {f_{BPF}}^n - 2\theta_{offset}\big) \\
&\quad + (\Delta L_s/L_s){M_{BPF}}^p{M_{BPF}}^n sin\big(4\theta_{err} \\
&\qquad + {f_{BPF}}^p + {f_{BPF}}^n + \pi - 2\theta_{offset}\big)\big]
\end{aligned}
\tag{8}
$$

By choosing

$$
\theta_{offset} = \frac{{f_{BPF}}^p + {f_{BPF}}^n}{2} \tag{9}
$$

equation (8) becomes an adequate error signal, because it equals zero only when the position is accurately estimated. As in section II, also here θ_{offset} is a function of motor speed and of the adopted BPF. Its values can be stored in a LUT. It is worth to underline that, with the proposed tracking observer, the phase relationship between high frequency voltages and currents does not affect position estimation and terms $\Delta\theta_{mot}$ and θ_{dgt} do not appear in (9).

IV. Experimental Results

The presented control scheme has been implemented on a SPM servomotor (500W, 6000 rpm, 1.9A, 2 pole pairs) using a dSPACE 1103 board. The sampling frequency of the control algorithm is 10 kHz, and the injection frequency is equal to 1 kHz. A picture of the test bench is reported in figure 3.

For the rotating voltage injection scheme, a second order BPF and a second order HPF are adopted, in order to limit the group delays and keep the implementation simple. The 3dB-attenuation frequencies of the BPF are 900 and 1100 Hz, while the 3dB-attenuation frequency of the HPF is 1kHz. For the pulsating voltage injection scheme, the same BPF and a first order LPF with cut-off frequency equal to 1000 Hz have been adopted. Figure 4 shows the magnitude and phase responses of the selected BP- and HP-filters.

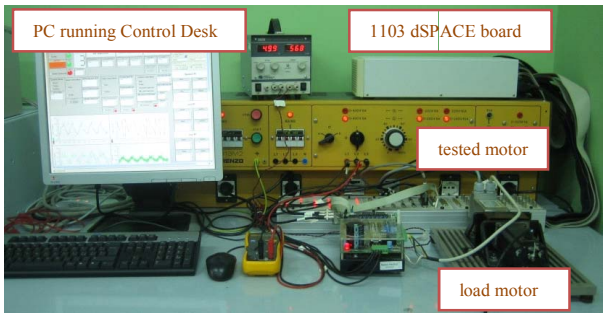

Figure 3 – Test bench.

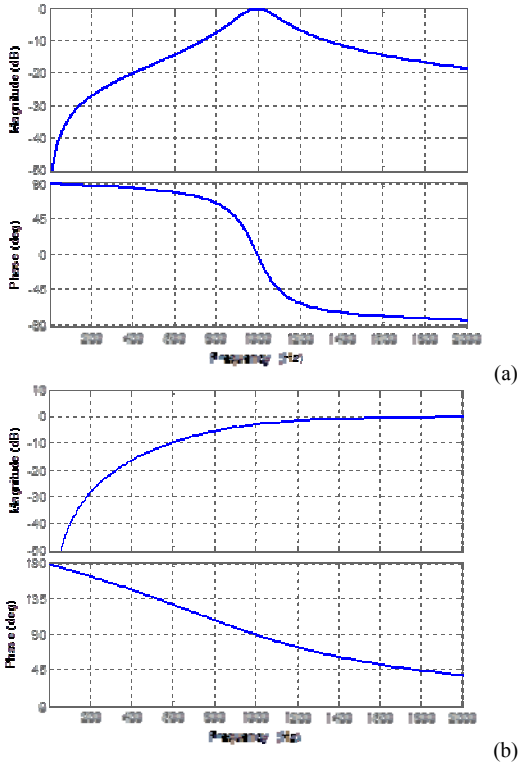

Fig. 4 – Magnitude and phase responses of BPF (a) and HPF (b)

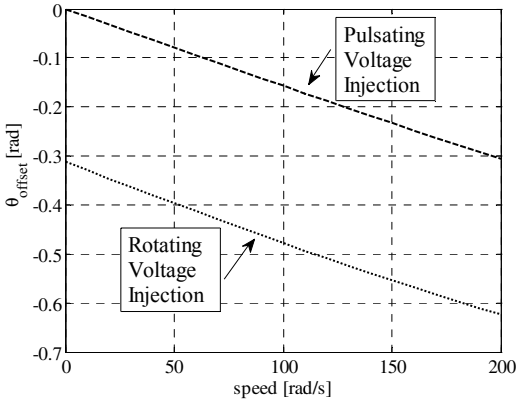

Fig. 5 – Comparison of the LUT used to compensate for position estimation errors due to filters.

The phase contribution of filters becomes very large in the medium to high speed range but cannot be neglected also in the very low speed range. Figure 5 reports the offset position as a function of the speed obtained for both the sensorless schemes with the considered sets of filters. A different choice of filters orders and cut-off frequencies can modify the results of figure 5, but in all practical cases the position offset due to filters is non negligible, as in the figure. The steady state average position estimation error has been measured under sensorless speed control in the speed range from zero to 200 rad/s. The results are reported in table I.

TABLE I. AVERAGE POSITION ESTIMATION ERRORS UNDER SPEED CONTROL AT STEADY-STATE

Speed [rad/s]	Rotating Voltage Injection Error [rad]		Pulsating Voltage Injection Error [rad]	
	NO LUT	*LUT*	*NO LUT*	*LUT*
0	0,34	-0,03	0,01	-0,05
10	0,33	0,01	0,08	-0,04
20	0,36	0,00	0,21	-0,03
30	0,37	-0,01	0,32	-0,03
40	0,38	-0,01	0,45	-0,03
50	0,40	0,00	0,66	-0,03
60	0,42	0,02	/	-0,03
70	0,45	0,02	/	-0,04
80	0,46	0,03	/	-0,04
90	0,48	0,03	/	-0,04
100	0,50	0,03	/	-0,04
110	0,52	0,03	/	-0,04
120	0,53	0,04	/	-0,05
130	0,55	0,03	/	-0,05
140	0,56	0,03	/	-0,05
150	0,58	0,03	/	-0,05

At very low speed, without compensation of θ_{offset}, the scheme based on pulsating injection guarantees lower errors. With this scheme the error increases rapidly with speed so that is is not possible to operate the drive above 50 rad/s. When the compensation of θ_{offset} is adopted, performances of both schemes are comparable.

A second set of experiments has been realized under torque control. The i_{sq} current reference is continuously changed from 0.5 A to -0.5 A and vice versa so to force the speed in the range between -70 rad/s and +70 rad/s. Figures 6 and 7 compare the drive performances obtained using rotating (fig.6) and pulsating (fig.7) voltage injection. In particular, the sensorless scheme was implemented with and without the compensation LUT, for the sake of comparison. The results with the two sensorless schemes are both very close to those of the sensored control, when LUT is adopted. On the contrary, they drastically worsen when the contribution of the filters is not compensated. The results shown in figures 8 and 9 lead to the same conclusion. In this case, the current control responses are visualized, in all the sensored and sensorless control modes considered so far: figure 8 refers to rotating voltage injection, while figure 9 refers to the pulsating voltage injection case. Finally, a position control scheme has been implemented using the rotating voltage injection scheme and the results, obtained with a two radians step reference, have been reported in figure 10. This results demonstrate that the effect of filters is also appreciable in the very low speed range, both in transients and steady state. When the LUT is adopted, the average estimation error at steady state is close to zero and this allows to control the rotor position with an average error below 0.04 electrical radians (1.15 mechanical degrees).

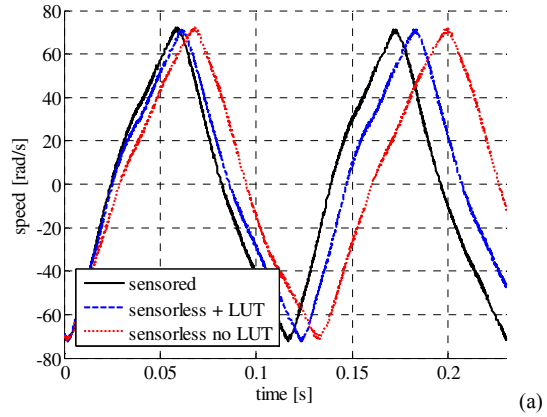

(a)

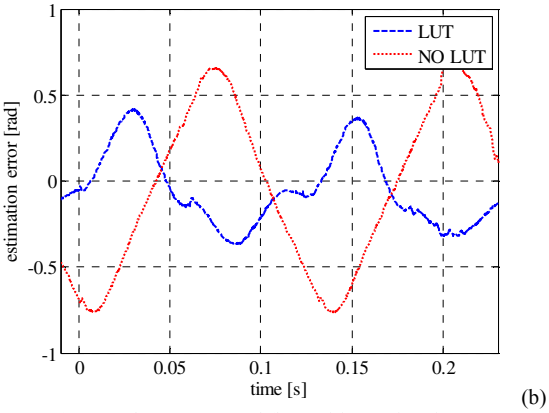

(b)

Figure 6 – (a) Speed responses and (b) position estimation errors under torque control using **rotating injection**.

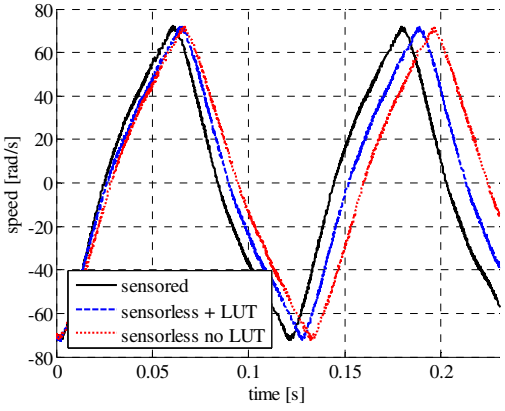

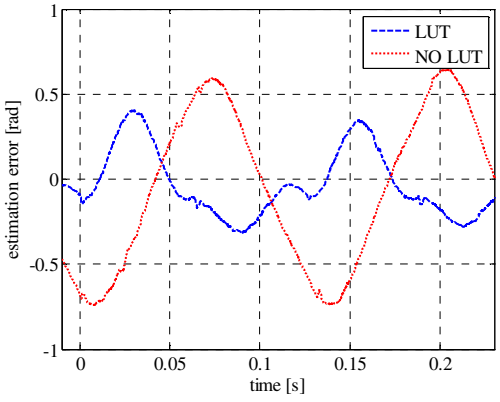

Figure 7 – (a) Speed responses and (b) position estimation errors under torque control using **pulsating injection**.

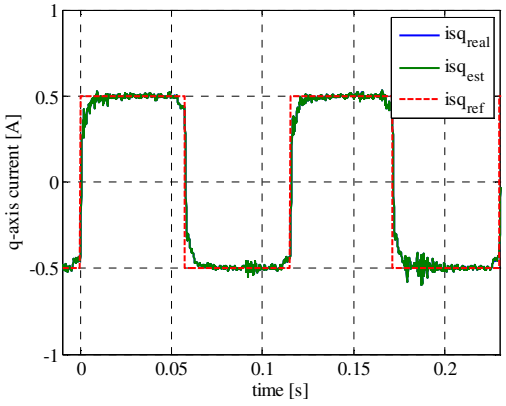

(a)

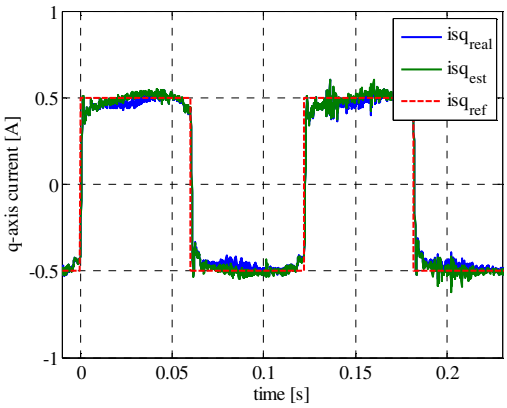

(b)

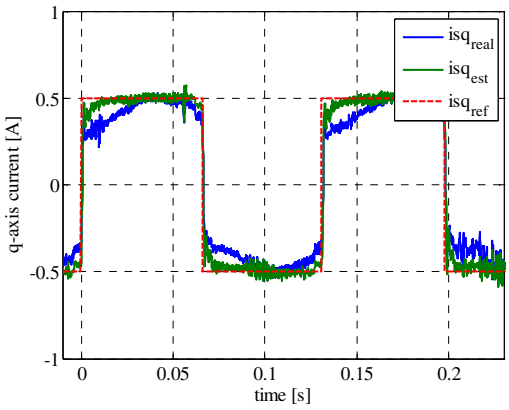

(c)

Fig. 8 – i_{sq} current responses using (a) sensored control, (b) sensorless control based on rotating voltage injection with the proposed compensation-LUT, and (c) sensorless control without compensation of the phase of the filters.

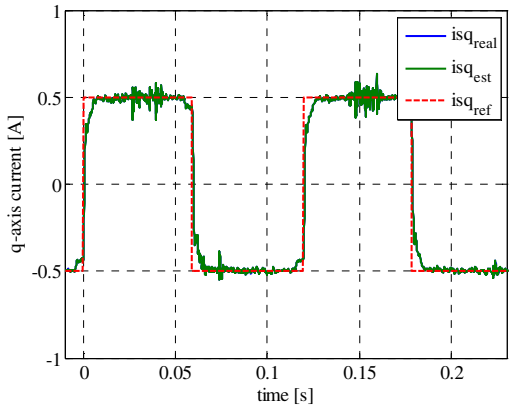

(a)

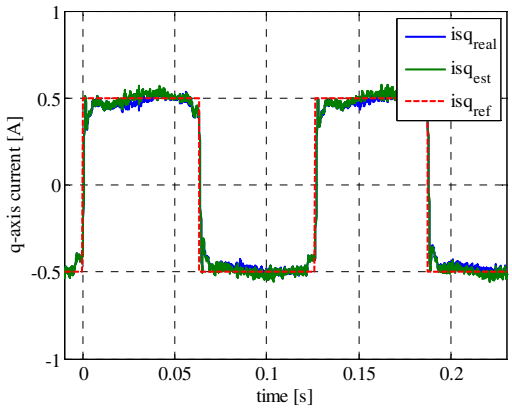

(b)

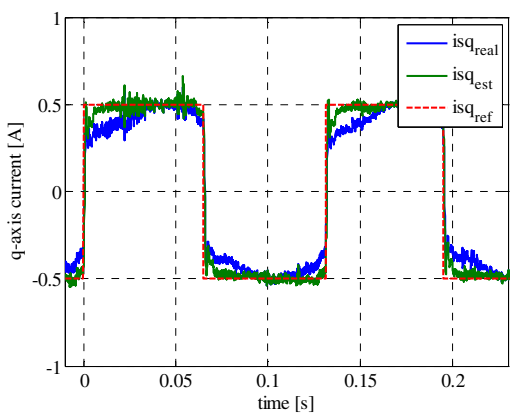

(c)

Fig. 9 – i_{sq} current responses using (a) sensored control, (b) sensorless control based on pulsating voltage injection with the proposed compensation LUT, and (c) sensorless control without compensation of the phase of the filters.

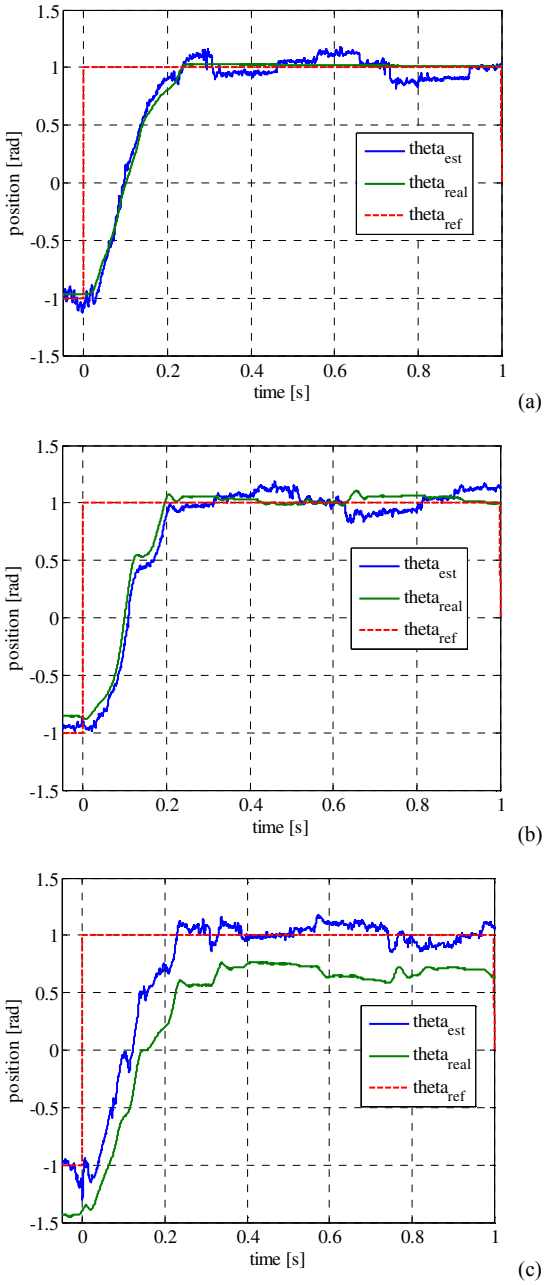

Fig. 10 – Position responses using sensored control (a), proposed sensorless control (b), sensorless control without compensation of the phase of the filters (c).

V. CONCLUSION

A study of the effects of non ideal filter responses and digital implementation on the tracking observers used for sensorless control of SPM motor drives has been presented. Carrier based sensorless control has been analyzed, in both cases of rotating and pulsating voltage injection. The position error due to all non idealities has been quantified analytically in the two cases, and feed-forward compensated via look-up tables, off-line calculated. The presented experimental results, referring to a small size servo-motor, confirm the accuracy of the analysis and the effectiveness of the proposed compensation strategy.

ACKNOWLEDGMENT

This work was partially funded by PON 2007-2013, Italian Ministry MIUR, project MALET code PON01_01693.

REFERENCES

[1] J. Holtz, “Sensorless control of induction machines - with or without signal injection?”, IEEE Transactions on Industrial Electronics, Volume 53, Issue 1, Feb. 2006, pp. 7 – 30.

[2] P. L. Jansen and R. D. Lorenz, “Transducerless position and velocity estimation in induction and salient AC machines,” IEEE Trans. Ind. Appl., vol. 31, no. 2, pp. 240–247, Mar./Apr. 1995.

[3] Y. Yoon, S. Sul, S. Morimoto, K. Ide, “High-Bandwidth Sensorless Algorithm for AC Machines Based on Square-Wave-Type Voltage Injection”, IEEE Trans. Ind. Applicat., vol. 47, no. 3, pp. 1361-1370, May/June 2011.

[4] Consoli, G. Scarcella, and A. Testa, “Industry application of zero-speed sensorless control techniques for PM synchronous motors,” IEEE Trans. Ind. Appl., vol. 37, no. 2, pp. 513–521, Mar./Apr. 2001

[5] M. Linke, R. Kennel, and J. Holtz, “Sensorless position control of permanent magnet synchronous machines without limitation at zero speed,” in Proc. 28th IEEE IECON, 2002, vol. 1, pp. 674–679.

[6] Jung-Ik Ha; Seog-Joo Kang; Seung-Ki Sul; , “Position-controlled synchronous reluctance motor without rotational transducer,”Industry Applications, IEEE Transactions on, vol.35, no.6, pp.1393-1398, Nov/Dec 1999

[7] H. Kim and R.D. Lorenz, “Carrier signal injection based sensorless control methods for IPM synchronous machine drives”, Conference Record of the 2004 IEEE Industry Applications Conference, 2004. 39th IAS Annual Meeting. Vol. 2, 3-7 Oct. 2004 Page(s):977 – 984.

[8] Raca, D.; Garcia, P.; Reigosa, D.D.; Briz, F.; Lorenz, R.D.; , "Carrier-Signal Selection for Sensorless Control of PM Synchronous Machines at Zero and Very Low Speeds," Industry Applications, IEEE Transactions on , vol.46, no.1, pp.167-178, Jan.-feb. 2010

[9] F. Cupertino, P. Giangrande, L. Salvatore, G. Pellegrino: “Sensorless position control of permanent magnet motors with pulsating current injection and compensation of motor end-effects”, IEEE Transactions on Industry Applications, Vol. 47, n. 3, 2011, pp. 1371-1379.